Received: 26 April 2021 | Revised: 20 June 2021 | Accepted: 28 June 2021

DOI: 10.1002/app.51373

ARTICLE

Applied Polymer SCIENCE WILEY

Influence of the dispersion of Nanoclays on the cellular structure of foams based on polystyrene

Alberto Ballesteros[1] | **Ester Laguna-Gutierrez**[2] | **Paula Cimavilla-Roman**[1] | **Maria Luisa Puertas**[3] | **Antonio Esteban-Cubillo**[3] | **Julio Santaren**[3] | **Miguel Angel Rodriguez-Perez**[1]

[1]Cellular Materials Laboratory (CellMat), Universidad de Valladolid, Valladolid, Spain

[2]CellMat Technologies S.L., Valladolid, Spain

[3]Tolsa SA, Madrid, Spain

Correspondence
Alberto Ballesteros, Cellular Materials Laboratory (CellMat), Universidad de Valladolid, Valladolid 47011, Spain.
Email: albalag93@gmail.com, albalag@fmc.uva.es

Funding information
Consejería de Educación, Junta de Castilla y León, Grant/Award Number: VA202P20; Ente publico regional de la energia de castilla y leon; Ministerio de Ciencia, Innovación y Universidades, Grant/Award Number: RTI2018-098749-B-I0

Abstract

In the present work blends of polystyrene (PS) with sepiolites have been produced using a melt extrusion process. The dispersion degree of the sepiolites in the PS has been analyzed by dynamic shear rheology and X-ray micro-computed tomography. Sepiolites treated with quaternary ammonium salts (O-QASEP) are better dispersed in the PS matrix than natural sepiolites (N-SEP) or sepiolites organo-modified with silane groups (O-SGSEP). A percolated network is obtained when using 6.0 wt% of O-QASEP, 8.0 wt% of N-SEP and 10.0 wt% of O-SGSEP. It has been shown that multiple extrusion processes have a negative effect on the polymer architecture. They produce a reduction in the length of the polymeric chains, and they do not lead to a better dispersion of the particles in the polymer matrix. Foams have been produced using a gas dissolution foaming process, where a strong effect of the dispersion degree on the cellular structure of the different foams was found. The effects on the cellular structure obtained by using different types of sepiolites, different contents of sepiolites and different extrusion conditions have been analyzed. The foams produced with the formulations containing O-QASEP present the lowest cell size and the most homogeneous cellular structures.

KEYWORDS

composites, foams, nanoparticles, nanowires and nanocrystals, polystyrene, rheology

1 | INTRODUCTION

Polystyrene (PS) foams are the second largest component of the foam market, after polyurethane (PU) foams, thanks to their low thermal conductivity, lightweight, high compressive strength, high resistance to moisture and medium to high tensile strength.[1,2] Among the different varieties of PS foams expanded PS (EPS) or extruded PS (XPS) are the used as thermal insulators. The possibility of using CO_2 as the primary blowing agent to produce XPS foams, replacing ozone-depleting blowing agents (fluorocarbons or chlorofluorocarbons), has conferred PS foams a privileged place in the thermal insulation market.[2] For XPS foams with densities around 30 kg/m^3 the thermal conductivity varies between 33 and 35 mW/mK, which is still higher than the thermal conductivity of

rigid PU foams (around 23–26 mW/mK, for the same density).[3]

A strategy to improve the thermal, electrical and mechanical properties of foams consists of incorporating nanoparticles into the polymer matrix.[4–6] The blending of polymeric foams and functional nanoparticles generates a class of materials known as cellular nanocomposites. Cellular nanocomposites combine the advantages of having a cellular structure with the multifunctional effects provided by the nano-particles.[7] On the one hand, particles have an important effect on the microscale properties, improving characteristics of the cellular structure and consequently, they also have a macroscopic effect on some physical properties like thermal or mechanical ones.[5,8] Nucleation can be modified by the presence of a small amount of well-dispersed nanoparticles leading to lower cell sizes and higher cell nucleation densities.[9] Furthermore, nanoparticles can also modify the extensional rheological properties of the polymer matrix, which have an important effect on the degeneration mechanisms and, as a consequence, on the cell size, cellular structure homogeneity and foam density.[10–12] Chen et al. demonstrated that foams with regular and homogeneous cellular structures present improved mechanical properties.[13] Moreover, it is known that thermal conductivity strongly depends on some parameters of the cellular structure such as cell size or porosity.[11] Therefore, nanoparticles could change the thermal aspects of the foams dramatically by decreasing considerably their thermal conductivity.[12]

The effects of incorporating nanoparticles into PS foams have been analyzed by several authors. Zhang et al. showed that the thermal insulation performance of PS foams was improved when introducing activated carbon nanoparticles.[14] Han et al. showed that nanoclays in a PS matrix it was possible to produce foams with lower cell sizes and higher cell densities. These cellular composites exhibited higher tensile modulus, better fire retardance, and better barrier properties than the pure PS foam.[15] Kaynak et al. demonstrated that the inclusion of just 5% of montmorillonites combined with some usual phosphate flame retardants produced a synergistic effect leading to a reduction of the flammability of the polymer.[16] Finally, Shen et al. claimed that the incorporation of carbon nanofibers to PS foams created a protective layer around the cell walls that resulted in the enhancement of foam strength.[17]

However, research efforts are still necessary to thoroughly understand the role of nanoparticles and the importance of having a suitable dispersion to obtain the desired properties. Only when the dispersion degree of the particles in the polymeric matrix is optimal, it is possible to increase the cell density and reduce the cell diameter, with respect to the pure polymeric foams.[18]

Due to the role that nano-particles play in the microscopic and macroscopic properties it is not difficult to understand why they have aroused a large interest in the scientific community.[19–22] Most of the papers dealing with nano-particles are based on the use of particles with spherical or layered morphologies.[13] For example, montmorillonites, silica or nano-porous silica particles have been widely used in PS foams.[23–25] However, it is not simple to find in literature studies analyzing the effects that needle-like shape particles, like sepiolites, have on the final structure of foams.[21,26–29] In fact, only one conference paper has been found. In this work, Notario et al. reported that it was possible to reduce, in a 60%, the cell size of PS foams by adding 0.5 wt% of sepiolites.[30] However, this paper does not provide a systematic study of how the dispersion degree of these particles affects the cellular structure of the foams.

Among all the needle-like shape particles available, sepiolites have been selected for this research work due to several reasons. On the one hand, sepiolites ($Si_{12}Mg_8O_{30}(OH)_4(OH_2)_4{\cdot}8H_2O$), which are natural fibrous clays, present outstanding sorption and rheological properties.[31,32] On the other hand, the structural characteristics of sepiolites favor their dispersibility in the polymer matrix. The structure of sepiolites consists of blocks of two tetrahedral silica sheets sandwiching an octahedral sheet of magnesium oxide-hydroxide (more information about the structure of the sepiolites can be found in the work of Tian et al.[33]).The dimensions of the cross-section tunnels are about 0.36 nm × 1.1 nm. The discontinuity of the silica sheets allows the presence of a significant number of silanol (Si–OH) groups on the surface of the particles. The existence of silanol groups can enhance the interfacial interaction between the nanoparticles and the polymer and therefore, they could help to improve the dispersion of the sepiolites in the polymeric matrix. Finally, due to their high aspect ratio (thicknesses in the nanometric scale, between 20 and 30 nm, average particle length ranging among 1 and 2 μm and large surfaces areas ~300 m^2/g), sepiolites are very interesting particles for being used as cell nucleating agents in thermoplastic foams. Bernardo et al. concluded that when incorporating 1.5 wt% of sepiolites organomodified with quaternary ammonium salts in a matrix of polymethyl methacrylate (PMMA) the cell size decreases by a factor of five and the cell nucleation density increases in a factor of 160.[21] Additionally, the inclusion of sepiolites can modify several properties of the polymer matrix like the behavior of the material against fire and its mechanical and thermal properties.[34–40]

The present work aims to analyze the dispersion of different types of sepiolites in a PS matrix as well as the effect of the dispersion degree on the cellular structure of PS foams produced by a gas dissolution foaming process. This

systematic study has been performed by evaluating, on the one hand, the importance of modifying the surface of sepiolites to ensure a proper interaction between the particles and polymer. For this purpose, natural sepiolites and sepiolites organo-modified with quaternary ammonium salts and silanol groups have been considered. The selection of quaternary ammonium salts and silanol groups was performed considering the results obtained in previous works in which both treatments were used to improve the interaction between these particles and a polymer matrix.[21,41–43] On the other hand, composites containing different amounts of sepiolites have been produced to evaluate the influence of the content of sepiolites on the dispersion degree and to determine the percolation threshold. Finally, different extrusion conditions have been used to produce the PS based composites. In particular, the number of extrusion cycles has been modified. Finally, the composites produced with 6 wt% of sepiolites have been foamed by the gas dissolution foaming process. The cellular structure of these foamed samples has been analyzed and the obtained results have been related to the results obtained after the dispersion analysis.

2 | EXPERIMENTAL

2.1 | Materials

A commercial PS, recommended for foam applications, (INEOS, Styrolution PS153F) with a melt flow index of 7.5 g/10 min (200°C/5 kg) and a glass transition temperature (Tg) of 102°C was used as polymer matrix. Three kinds of sepiolites, kindly supplied by Tolsa S.A. (Madrid, Spain), were used in this work. They can be distinguished between non-organically modified sepiolites (labeled as N-SEP), sepiolites organically modified with quaternary ammonium salts (O-QASEP) and sepiolites organically modified with silanol groups (O-SGSEP). An antioxidant (BASF, Irganox 1010) was also used to reduce thermal degradation during the extrusion stage.

2.2 | Production process

A wet milling process was used to obtain separated sepiolites from the starting sheaf-form in which particles appear naturally. The procedure of the wet milling and surface treatment of the particles was performed as it was described in a previous work.[43]

Before the extrusion process, the materials were dried in a vacuum oven (Mod. VacioTem TV, P-Selecta) at 70°C for 4 h, in the case of pure PS, and at 80°C for 8 h in the case of the different types of sepiolites. The mixing of the polymer with the sepiolites was carried out in a twin-screw extruder (Collin ZK 25 T with L/D of 24) following a temperature profile that goes from 145 to 185°C (at the die of the extruder) and with a screw rate of 50 rpm. Some amount of this material was re-extruded, once again, under the same conditions, to analyze how the number of extrusion cycles affects the dispersion of the sepiolites in the PS matrix. The pure PS was also submitted to different extrusion cycles to analyze how the rheological behavior of the polymer is affected by the extrusion process. The different formulations produced in this work are shown in Table 1. Formulations containing 2, 6, 8, and 10 wt% of the different types of sepiolites were fabricated to evaluate the effects of changing the content of the particles in their dispersibility.

The different formulations were later thermoformed in a hot-cold plate press to obtain materials with the desired shape and size. The compression molding process was carried out at a temperature of 235°C and at a pressure of 27 bars.

The foaming of the samples was carried out using the solid-state gas dissolution foaming method.[44] For this purpose, a high-pressure vessel (model PARR 4681), provided by Parr Instrument Company, with a capacity of 1 L and capable of operating at a maximum temperature of 350°C and at a maximum pressure of 41 MPa was used. The reactor is equipped with a pressure pump controller (model SFT-10), provided by Supercritical Fluid Technologies Inc., which is controlled automatically to keep the pressure on the desired values. The pressure vessel is also equipped with a clamp heater of 1500 W where the temperature is controlled via a CAL 3300 (from CAL controls) temperature controller. The foaming process was performed in two steps.[45] Samples were firstly introduced in the pressure vessel at 8 MPa of CO_2 pressure for the saturation stage. The saturation temperature was 40°C and the saturation time was 24 h. It was experimentally proved that this time is enough to achieve full saturation of CO_2 in PS at the conditions under study. After saturation, the pressure was abruptly released. Finally, for the foaming stage, samples were removed from the pressure vessel and introduced in a thermostatic silicon bath at 120°C for 1 min. The time between the release of the pressure and the immersion in the thermal bath was 2 min. Once the materials were expanded, they were cooled down in water to stabilize their cellular structure.

2.3 | Characterization

2.3.1 | Dynamic shear measurements

A shear stress-controlled rheometer (AR 2000 EX from TA Instruments) was used to measure the dispersion degree of the different formulations. Dynamic shear measurements were conducted at a temperature of 220°C,

TABLE 1 Formulations produced and characterized during the present study

Sample name	Content of polymer (wt%)	Content of Sepiolites (wt%)	Content of antioxidant (wt%)
Pure PS	99.5	0.0	0.5
PS + 2% N-SEP	97.5	2.0	0.5
PS + 2% O-QASEP	97.5	2.0	0.5
PS + 2% O-SGSEP	97.5	2.0	0.5
PS + 6% N-SEP	93.5	6.0	0.5
PS + 6% O-QASEP	93.5	6.0	0.5
PS + 6% O-SGSEP	93.5	6.0	0.5
PS + 8% N-SEP	91.5	8.0	0.5
PS + 8% O-QASEP	91.5	8.0	0.5
PS + 8% O-SGSEP	91.5	8.0	0.5
PS + 10% N-SEP	89.5	10.0	0.5
PS + 10% O-QASEP	89.5	10.0	0.5
PS + 10% O-SGSEP	89.5	10.0	0.5

Note: All formulations have been subjected to one and two extrusion cycles.

under a nitrogen atmosphere, and using 25 mm diameter parallel plates. A fixed gap of 1 mm was selected to perform the rheological measurements.

First a strain sweep test, at a fixed dynamic frequency (1 rad s^{-1}), was performed to determine the linear viscoelastic regime of the different nanocomposites. Later, a time sweep was performed to recover the initial state of the particle network, which was partially deformed when the sample was loaded in the rheometer. The duration of the time sweep varied between 360 and 600 s, depending on the material. Finally, the frequency sweep step was performed, in a range of angular frequencies varying between 0.01 and 100 rad s^{-1}. From these measurements, four parameters were analyzed: dynamic shear viscosity ($|\eta^*|$), storage modulus ($(G'(\omega))$), loss modulus ($(G''(\omega))$) and crossover frequency (ω_x). Furthermore, the Mark-Houwink Sakurada equation, which relates the complex viscosity with the molecular weight, was used to estimate the molecular weight of the polymer matrix.[46]

2.3.2 | X-ray micro-computed tomography

The set-up employed to perform the micro-computed tomography experiments consisted of a micro-focus cone-beam X-ray source L10101 from Hamamatsu (spot size: 5 μm, voltage: 20–100 kV, current: 0–200 μA) with a maximum output power of 20 W and a high sensitivity flat panel detector C7940DK-02 also from Hamamatsu (2240 × 2344 pixels, 50 μm of pixel size). In addition, a rotation stage was mounted on a linear stage which enables movement between the source and detector and permits varying the magnification factor.[47]

The linear stage was placed in a position so that the magnification value was ×20, leading to a pixel size of 2.5 μm. A tube voltage of 55 kV and a current of 170 μA were selected for the measurements. The detector exposure time was 1000 ms and the rotation step was 0.3°. To enhance the contrast in the reconstructed images, each projection was the result of integrating three consecutive images.

Once all the projections were acquired, the reconstruction process of the tomogram was carried out using Octopus, server/client reconstruction package.[48]

Due to the limited spatial resolution of the tomographic system (2.5 μm), the reconstructed slices can be used to analyze the number of agglomerates of particles present in the solid PS nanocomposites. The isolated sepiolites present sizes that are between 1 and 2 μm and with this X-ray experiment only particles with sizes higher than this 2.5 μm can be detected. Therefore, the particles observed in this experiment are agglomerations of the primary sepiolites particles. This method to determine the agglomerates of sepiolites has been applied in other works, like the one performed by Bernardo et al.[49]

To calculate the number of agglomerates of particles, a tomographic volume of 1.25 × 2.50 × 3.50 mm^3 has been considered. Firstly, two consecutive 3D filters have been applied in the reconstructed slices. In addition, a 3D median filter (two pixels of radius) has been applied to remove noise from the images and later, a 3D maximum filter (one pixel of radius) has been computed to enhance the particles gray level intensity. Then, the particles have been binarized by means of a thresholding process based on the different level of absorption between polymer and fillers. The percentage of agglomerates in the sample has been calculated according to (Equation (1)), by

measuring the volume fraction occupied by the agglomerates ($\%V_{sep}$) and considering the real mass fraction of particles in the sample ($\%m_{sep}$).

$$\text{Agglomerates}\,(\%) = \frac{\frac{\rho_{sep}\cdot \%V_{sep}}{\rho_{solid}}}{\%m_{sep}}, \tag{1}$$

where ρ_{sep} is the theoretical density of the sepiolites (2.1 g/cm^3) and ρ_{solid} represents the density of the solid nanocomposite, which was measured by gas pycnometry.

2.3.3 | Gas uptake

The gravimetric method has been used to measure the gas absorbed during the saturation stage. By using this method, the gas absorbed is obtained directly from determining the weight gain by the polymer sample during the sorption stage. It consists of calculating the ratio between the difference in the sample weight before and after the saturation process and the initial weight of the composite. This ratio provides the percentage of the CO_2 absorbed by the composite, as can be seen in (Equation (2)).

$$CO_{2\,\text{Uptake}} = \frac{W_s - W_0}{W_0}, \tag{2}$$

where W_s is the weight after saturation and W_0 is the initial weight.

2.3.4 | Density

The density of the solid precursors was analyzed using a gas pycnometer (Accupyc II 1340 from Micromeritics). The density of the cellular materials, which were produced using the gas dissolution foaming process, was determined by the geometric method, that is, dividing the corresponding mass of each specimen by its geometric volume (ASTM standard D1622-08). The foamed samples used to determine the density have a cylindrical shape with a diameter of 7.5 cm and a thickness of 6 mm. The following equations (Equations (3) and (4)) show the way of determining the relative density (ρ_r) and expansion ratio (E). Relative density is defined as the ratio between the density of the foam (ρ_{foam}) and the density of the bulk solid material (ρ_{solid}). On the other hand, the expansion ratio is defined as the inverse of the relative density.

$$\rho_r = \frac{\rho_{foam}}{\rho_{solid}}, \tag{3}$$

$$E = \frac{1}{\rho_r}. \tag{4}$$

2.3.5 | Open cell content

To evaluate the open cell content of the samples, according to the Standard ASTM D6226-10, see (Equation (5)), a gas pycnometer Accupyc II 1340 from Micromeritics was used.

$$OC(\%) = 100\left(\frac{v_{geometric} - v_{pycnometer}}{p.V_{geometric}}\right), \tag{5}$$

where $v_{geometric}$ is the geometric volume of the sample, $v_{pycnometer}$ is the volume of the sample obtained with the pycnometer and p is the porosity calculated as $\left(1-\frac{\rho_{foam}}{\rho_{solid}}\right)$.

2.3.6 | Cellular structure

The structure of the cellular materials, produced by gas dissolution foaming, was analyzed with a scanning electron microscope (SEM) (Jeol, Mod. JSM-820). Parameters such as the average cell size (Φ), and the cell nucleation density (N_0) were analyzed with an image processing tool based on the software Fiji/Image J.[50] More than 100 cells of different regions of each cellular material have been considered to determine these parameters.

The average cell size is defined as it is indicated in (Equation (6)).

$$\phi = \sum_{i=1}^{n}\frac{\phi_i}{n} = \sum_{i=1}^{n}\frac{cf}{2n}\left(\phi_x^i + \phi_y^i\right), \tag{6}$$

where n is the total number of cells counted in the image, ϕ_i is the three-dimensional value of the cell size for and specific cell. ϕ_x^i and ϕ_y^i are the chord lengths of the cells in the directions x and y, respectively and cf is a correction factor used to convert the two-dimensional value of the cell size to a three-dimensional value. As it was indicated in the work of Pinto et al. a value of 1.273, has been selected for the mentioned correction factor.[50]

The cell nucleation density (N_0), defined as the number of cells per unit volume of the solid, was obtained using the Kumar's theoretical approximation represented in (Equation (7)).[45] In this formula N_v is the cell density, defined as the number of cells per cubic centimeter of the foamed material, and ρ_r is the relative density (see Equation (3)).

$$N_0 = \frac{N_v}{\rho_r}. \quad (7)$$

In this work, the cellular materials containing sepiolites present a bimodal structure showing small cells, combined with large cells, those with a size higher than 200 μm. Although, the number of large cells is lower than the number of small cells, the volume occupied by the large cells is not negligible. For this reason, to quantify the observed bimodality the relative volume fraction occupied by the small cells is defined as it is indicated in (Equation (8)).

$$v_s = 100 \cdot \frac{A_t - A_l}{A_t}, \quad (8)$$

where A_l is the observed area occupied by the large cells in the SEM images and A_t the total area of the image. In the pure PS foams, which do not present a bimodal structure, this parameter was not calculated, and it was considered as zero.

Finally, the ratio between the standard deviation of the cell size (SD) and the average value of the cell size (SD/Φ), allows analyzing the homogeneity of the cellular structure. Low values of this parameter are related to a homogeneous cellular structure with a narrow cell size distribution.

Only the small cells were considered for the determination of the different parameters: cell size, cell nucleation density and SD/Φ.

3 | RESULTS

3.1 | Analysis of the dispersion degree by shear rheology

The values of the zero-shear viscosity, the slopes of the storage modulus and loss modulus and the number of crossover points between the curves corresponding to the loss and storage moduli have been analyzed for the different formulations.

3.1.1 | Effects of the type of particles

In this section, the study is focused on materials produced with different types of sepiolites: N-SEP, O-QASEP, and O-SGSEP. Therefore, for comparative purposes, the content of particles has been fixed (6 wt%) as well as the production conditions (one single extrusion cycle).

Figure 1 shows the behavior of the complex viscosity ($|\eta^*|$), the storage modulus ($G'(\omega)$), and the loss modulus ($G''(\omega)$) as a function of the angular frequency for the pure PS and for the three types of composites. Figure 1(a) shows an increase in the complex viscosity values of the formulations containing sepiolites with respect to the pure PS. This increment is chiefly remarkable in the formulation containing O-QASEP. Moreover, in this composite the Newtonian plateau, observed with the other materials at low frequencies, disappears and the behavior corresponds to that of a non-Newtonian power law material.

For the materials presenting a Newtonian-plateau, the zero-shear viscosity (η_0) is determined as the value of the viscosity in the Newtonian-plateau. The results of zero-shear viscosity are collected in Table 2. Results indicate that the composites present a higher zero-shear viscosity than the pure PS.

Storage modulus ($G'(\omega)$) is altered by variations in the molecular structure of polymers. At low frequencies, in the area called terminal region, where the longest relaxation times play a major role, the storage modulus is usually proportional to the square of the frequency $G' \propto \omega^2$.[51] To quantify the changes in the storage modulus, the slopes of the G' curves in the terminal region (between 0.01 and 0.1 rad/s) were measured. The obtained results are collected in Table 2. For the pristine polymer, it is expected that the slope of G' presents a value close to 2. As soon as the density of particles increases, the slope should approach to 1. Finally, when the formulations are reaching the percolation state or they are completely percolated, the slope of G' should present values approaching to 0.[52] It is important to mention that the density of particles can increase due to two main reasons. On the one hand, the density of particles increases if the content of particles introduced in the polymeric matrix increases. On the other hand, the density of particles increases if the content of particles is fixed but the particles are dispersed in a more efficient way. Therefore, in systems in which the number of particles is fixed, a reduction of the slope of G' is related with an increment of the dispersion degree. Figure 1(b) shows the differences between the curves of the formulations containing particles and that of the pure polymer. These differences are mainly remarkable in the slopes of the curves in the terminal region, which are clearly reduced in the systems containing particles. A reduction of 29% of the slope of G' is achieved when adding 6 wt% of N-SEP. Meanwhile, a reduction of the slopes of G' of 62% and 26% is obtained when adding 6 wt% of O-QASEP and 6 wt% of O-SGSEP, respectively. Furthermore, as it is indicated in Table 2, the slope of G' corresponding to the composite containing 6 wt% of O-QASEP particles presents a value close to 0, which indicates that, for this kind of sepiolites, this content is close to the percolation threshold.

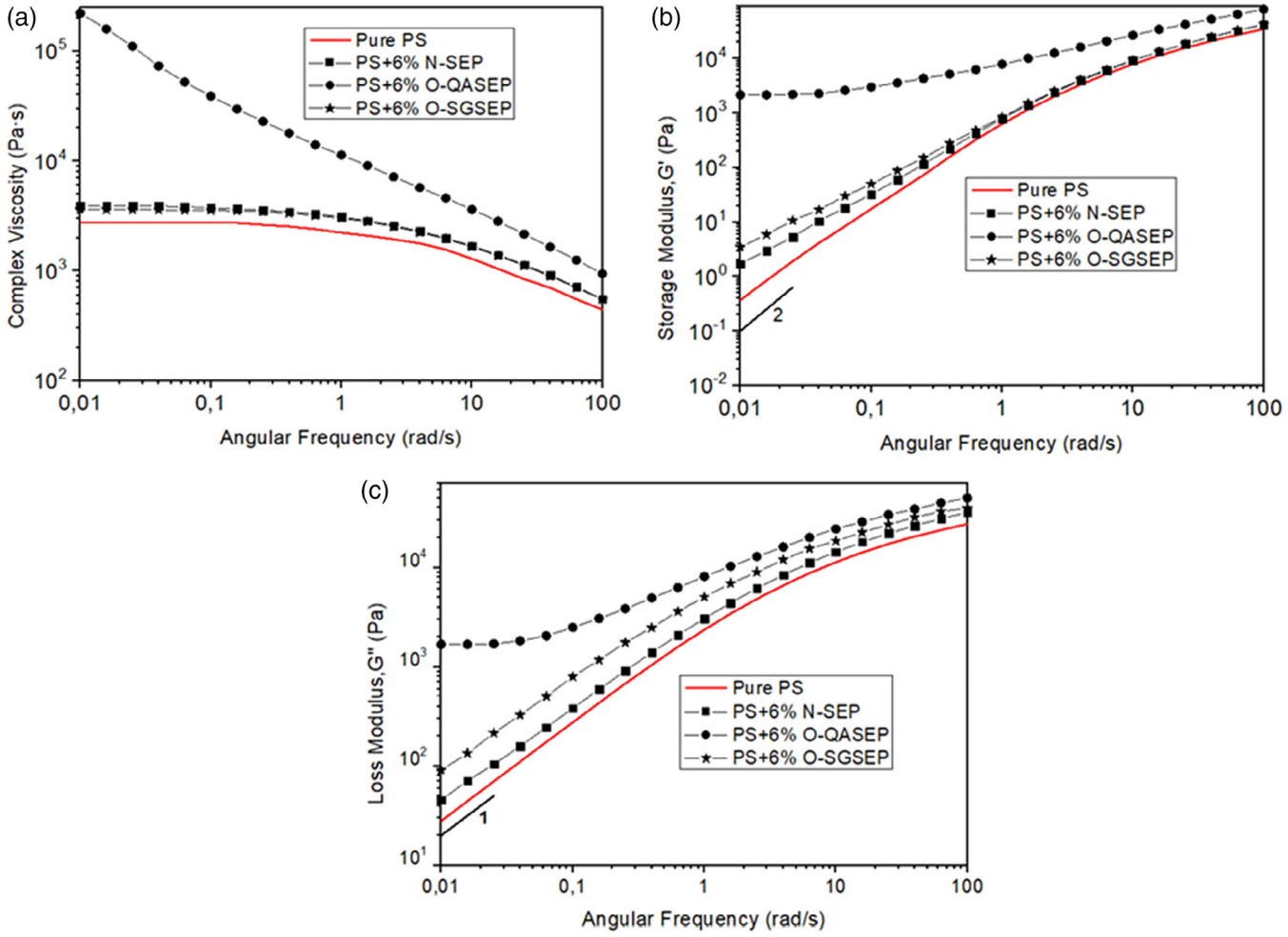

FIGURE 1 Viscoelastic properties for the pure PS and the different composites produced with a fixed content of sepiolites (6 wt%). All formulations were produced using one single extrusion cycle. (a) Complex viscosity versus angular frequency. (b) Storage modulus versus angular frequency. (c) Loss modulus versus angular frequency. Common slopes values for a pure polymer are also shown in (b, c) [Color figure can be viewed at wileyonlinelibrary.com]

TABLE 2 Linear viscoelastic properties of the pure PS and the different composites containing 6 wt% of different types of sepiolites, all of them subjected to a single extrusion process

Sample name	Zero shear viscosity, η_0 (Pa s)	Slope of G' (Pa s)	Slope of G'' (Pa s)	Crossover frequency, ω_x (rad/s)
Pure PS	2905	1.78	0.96	42.29
PS + 6% N-SEP	3839	1.27	0.95	41.18
PS + 6% O-QASEP	Non-Newtonian	0.67	0.75	3.67/28.67
PS + 6% O-SGSEP	3498	1.32	0.92	42.16

On the other hand, the loss modulus, $G''(\omega)$, of a pure polymer should be proportional to the frequency in the terminal region $G'' \propto \omega$.[51] The effect of the type of particles in the loss modulus is shown in Figure 2(c). The slopes of G'' in the terminal region have been also calculated and the obtained values are shown in Table 2. The slopes of G'' for the systems containing N-SEP or O-SGSEP are like that of the pure polymer. However, the value for the material containing O-QASEP is much lower. A reduction of 21% is reported indicating, once again, a much better dispersion of this type of particles in the PS matrix.

The crossover frequency (ω_x) has been also measured (see Table 2). This parameter is defined as the frequency at which the storage modulus $G'(\omega)$ and the loss modulus $G''(\omega)$ intersect. The presence of one single crossover

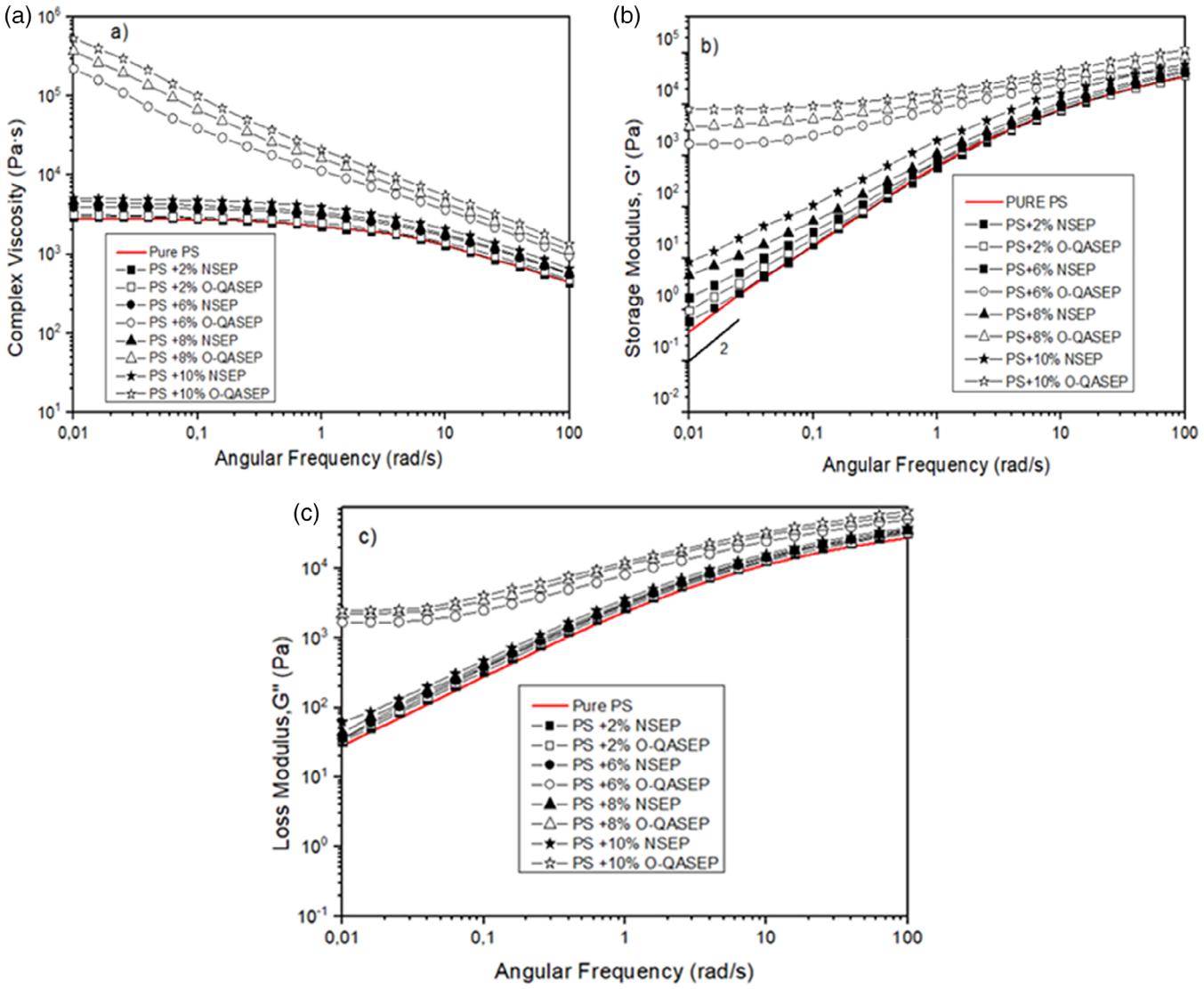

FIGURE 2 Viscoelastic properties for the pure PS and the blends of the polymer with different contents of N-SEP and O-QASEP. All the formulations were produced with one extrusion cycle. (a) Complex viscosity versus angular frequency. (b) Storage modulus versus angular frequency. (c) Loss modulus versus angular frequency. Common slopes values for a pure polymer are also shown in figures (b) and (c) [Color figure can be viewed at wileyonlinelibrary.com]

point indicates that the material is not already percolated.[52] On the other hand, the presence of two crossover points indicates that the density of particles is close to the percolation threshold. Finally, a spectrum in which no crossover points appear implies that the density of particles is higher than the percolation threshold.[52] The data collected in Table 2 show that the composites produced with 6 wt% of N-SEP and with 6 wt% of O-SGSEP only show a single crossover point, which indicates that in these materials a network structure has not been formed. Meanwhile, for the material produced with 6 wt% of O-QASEP two crossover points have been obtained, which indicates that this composite presents a percolated structure.

Furthermore, the crossover frequencies of the storage and loss modulus curves shift to lower frequencies thanks to the inclusion of particles. This behavior indicates that the composites remain in a solid-like behavior for a wider region of frequencies. In other words, the dynamic oscillatory shear measurements indicate that the incorporation of sepiolites to a PS matrix modifies the long-time relaxation behavior of the polymer by increasing the relaxation time due to the formation of a three-dimensional network structure.[53] Kotsilkova et al. suggested in their work that longer relaxation times indicate that the structure of the nanocomposite is creating a significant energetic barrier against the molecular motion during the shear flow.[54]

With all the information collected it is possible to conclude that only the formulation containing 6 wt% of O-QASEP is already percolated. Moreover, the rheological results also indicate that O-QASEP presents a much better dispersion degree. On the other hand, the formulations containing N-SEP and O-SGSEP exhibit a rheological behavior that is like that of the pure PS matrix, which indicates a poor dispersion of these particles in the polymer matrix.

3.1.2 | Effect of the content of particles

This section analyzes the effects on the rheological behavior produced by changing the content of particles. The percentages of particles introduced in the polymer are the following ones: 2, 6, 8, and 10 wt%. All the data showed in this section belongs to blends produced in a single extrusion process.

Figure 2(a) shows the effect of changing the content of particles on the complex viscosity. Only the particles which lead to the most promising results have been included in this figure, On the other hand, in Table 3, the data corresponding to the three types of particles are reported: N-SEP, O-QASEP, and O-SGSEP. For blends containing N-SEP, the complex viscosity slightly increases as the content of particles increases. For example, the zero-shear viscosity increases 0.3% and 32%, with respect to the pure PS, when incorporating 2 and 6 wt% of N-SEP, respectively. However, the presence of a non-Newtonian power law behavior in the terminal region is only observed when high amounts of particles are introduced in the system (8 and 10 wt%). On the other hand, the inclusion of O-QASEP, in percentages similar or higher than 6 wt%, leads to a significant modification of the structure of the material. Finally, with the O-SGSEP particles the viscosity increases 0.2%, 20%, and 62%, compared to the neat material, when introducing 2, 6, and 8 wt% of particles, respectively. Therefore, it is necessary to incorporate contents close to 10 wt% to create a percolated network when using these O-SGSEP particles. Due to the change perceived from a Newtonian to a non-Newtonian power law regime in the terminal region of complex viscosity and with the data collected in Table 3, it is possible to assert that the percolation state is reached when incorporating 6 wt% of O-QASEP, 8 wt% of N-SEP and 10 wt% of O-SGSEP.

Both the storage modulus, $G'(\omega)$, and loss modulus, $G''(\omega)$, increase when the content of particles increases, as it can be seen in Figure 2(b,c), respectively. From the values of the slopes of G' and G'', collected in Table 3, it is possible to conclude that the slopes decrease when the content of particles increases. For instance, a reduction of the slopes of G' of 53%, 62%, 91% and 97%, with respect to the pure PS, is reached for the formulations containing 2, 6, 8, and 10 wt% of O-QASEP, respectively. Furthermore, the slopes of the two moduli, in the terminal region, of the samples presenting a Newtonian plateau (2 and 6 wt% of N-SEP, 2 wt% of O-QASEP and 2, 6, and 8 wt% of O-SGSEP) are closed to 1. Moreover, the storage modulus and loss modulus of these last formulations intersect in a single crossover point, which indicates that in these materials a percolated network structure has not been formed. On the contrary, the formulations containing contents similar or higher than 6 wt% of O-QASEP, 8 wt% of N-SEP and 10 wt% of O-SGSEP present slopes of G' and G'' that approach to 0.

The theoretical percolation threshold (ϕ_{per}) has been determined. To obtain this parameter the following (Equation (9)) has been used.[55]

$$G' = C\left(\phi_c - \phi_{\text{per}}\right)^n, \tag{9}$$

where C is a constant, n is a power law exponent, ϕ_c is the clay volume fraction, ϕ_{per} is the percolation threshold volume fraction and G' is the value of the storage modulus at low frequencies. The value of ϕ_{per} is obtained by fitting to a linear regression the curve $\log(G')$ versus $\log\left(\phi - \phi_{\text{per}}\right)$. This procedure is done for different values of ϕ_{per}. This equation can be used only in the proximities of the percolation threshold.[56] Finally, the value of ϕ_{per} for which the best fit is obtained is considered as the percolation threshold of the composite. In the system that contains O-QASEP particles a value of the percolation threshold of 4.0 wt% was obtained. This value was 7.5 wt% for the system containing N-SEP and 9.0 wt% for the system containing O-SGSEP.

Finally, it is essential to mention that the crossover points between G' and G'' change from 1 single point to 2 points or even to 0 points depending on the type and content of particles. Table 3 summarizes this behavior. The formulations containing 2 and 6 wt% of N-SEP, 2 wt% of O-QASEP and 2, 6, and 8 wt% of O-SGSEP present only a single crossover point, which indicates that in these formulations the percolation threshold is not reached. Meanwhile, the formulations containing 8 wt% of N-SEP, 6 wt% of O-QASEP and 10 wt% of O-SGSEP present two crossover points and hence, it can be concluded that they are close to the percolation threshold. Finally, the materials containing 10 wt% of N-SEP and 8 and 10 wt% of O-QASEP do not present any crossover point, which indicates that these contents of particles are higher than the percolation threshold. Furthermore, when the particles are introduced in the polymer it is also possible to observe a shifting effect of the crossover point to lower frequencies. It is remarkable the shifting

TABLE 3 Linear viscoelastic properties of the pure PS and the composites containing 2, 6, 8, and 10 wt% of N-SEP, O-QASEP, and O-SGSEP

Sample name	Zero shear viscosity, η_0 (Pa s)	Slope of G' (Pa s)	Slope of G'' (Pa s)	Crossover frequency, ω_x (rad/s)
Pure PS	2905	1.78	0.96	42.29
PS + 2% N-SEP	2916	1.48	0.97	42.26
PS + 2% O-QASEP	2943	0.82	0.94	41.15
PS + 2% O-SGSEP	2912	1.52	0.98	42.89
PS + 6% N-SEP	3839	1.27	0.95	41.18
PS + 6% O-QASEP	Non-Newtonian	0.67	0.75	3.67/28.67
PS + 6% O-SGSEP	3498	1.32	0.92	42.16
PS + 8% N-SEP	Non-Newtonian	0.57	0.67	2.16/25.67
PS + 8% O-QASEP	Non-Newtonian	0.16	0.44	No crossover points
PS + 8% O-SGSEP	4726	1.15	0.89	39.24
PS + 10% N-SEP	Non-Newtonian	0.07	0.42	No crossover points
PS + 10% O-QASEP	Non-Newtonian	0.05	0.39	No crossover points
PS + 10% O-SGSEP	Non-Newtonian	0.46	0.54	2.15/23.14

Note: The composites were subjected to a single extrusion process.

of 13.62 rad/s in the case of the formulation containing 6 wt% of O-QASEP.

3.1.3 | Effects of the extrusion process

In this section, the effects on the dispersion degree associated to produce the composites by using one or two extrusion cycles are analyzed. Moreover, these effects have been also studied in the pure PS to analyze the importance of comparing materials with the same thermo-mechanical history.

Figure 3 shows the complex viscosity ($|\eta^*|$), the storage modulus ($G'(\omega)$) and the loss modulus ($G''(\omega)$) for the pure PS after zero (raw material as received), one and two extrusion cycles. Figure 3(a) shows the effect of the number of extrusion cycles on the complex viscosity. The material with the highest value of the zero-shear viscosity (η_0) is the one that has not been extruded. The zero-shear viscosity of the non-extruded pure PS material is 5% and 10% higher than that of the PS after one and two extrusion cycles, respectively (see Table 4). On the other hand, no important differences are detected between the curves of G' and G'', for the three PS samples.

Only in the terminal region, a slight difference is detected (see Figure 3(b,c)). The numerical values of the slopes in the terminal region are depicted in Table 4. Results indicate that the slopes are lower for the non-extruded pure polymer than for the ones subjected to one and two extrusion cycles. An increase of a 3% in the slope of G' is obtained when the material goes from 0 extrusion cycles to one or two extrusion cycles. This fact could indicate a possible deterioration of the molecular structure of the pure polymer due to the extrusion process. Results also indicate that when increasing the number of extrusions cycles the crossover point is shifted to higher frequencies. This variation in the frequency of the crossover points indicates that the material presents a lower solid-like behavior.

Typically, an increase in the molecular weight and in the molecular weight distribution results in an increment of the zero-shear viscosity value, in a reduction of the slopes of G' (ω) and $G''(\omega)$ and in an increment of the shear thinning behavior.[57] In the present study, when the number of extrusion cycles increases, the complex viscosity decreases, the values of the slopes of G' (ω) and $G''(\omega)$ increase and the shear thinning behavior also decreases. Furthermore, the molecular weight values, estimated by using the Mark-Houwink Sakurada equation, exhibit a slight reduction when the formulation is subjected to a higher number of extrusion cycles. Therefore, these results could be indicating that some degradation of the polymer molecular structure could occur during the extrusion process leading to a reduction of the lengths of the polymeric chains.

Although it was proven that a major number of extrusion cycles lead to some degradation of the pure polymer, in the case of the composites an increase in the number of extrusion cycles could lead to a better dispersion of the

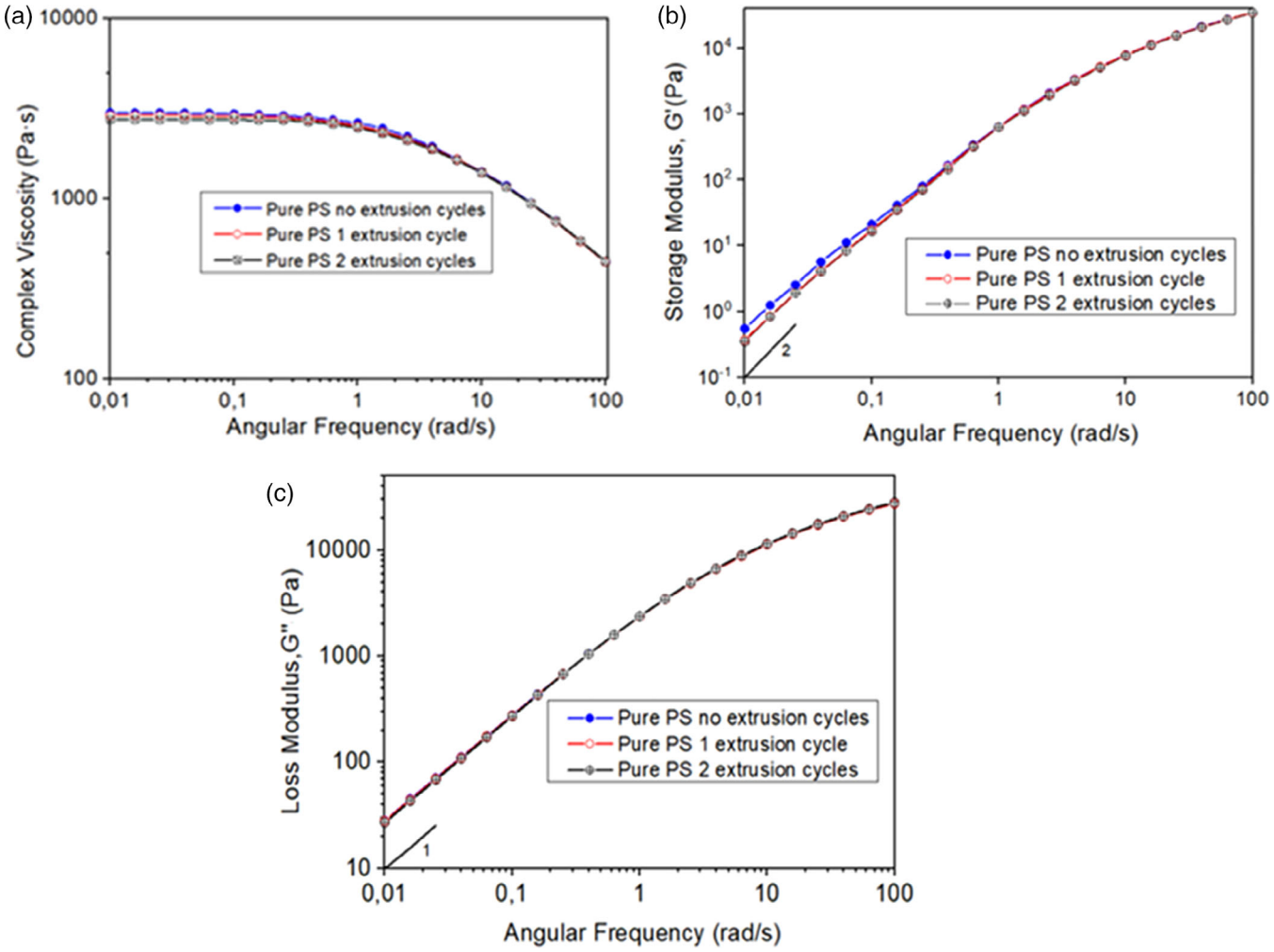

FIGURE 3 Viscoelastic properties for the pure PS subjected to different extrusion cycles. (a) Complex viscosity versus angular frequency. (b) Storage modulus versus angular frequency. (c) Loss of modulus versus angular frequency. Common slopes values for a pure polymer are also shown in figures (b) and (c) [Color figure can be viewed at wileyonlinelibrary.com]

TABLE 4 Linear viscoelastic properties of pure PS subjected to a different number of extrusion cycles

Sample name	Zero shear viscosity, η_0 (Pa s)	Slope of G' (Pa s)	Slope of G'' (Pa s)	Crossover frequency, ω_x (rad/s)	Molecular weight (g/mol)
Pure PS no extrusion cycles	3076	1.72	0.96	41.01	1.56 E+05
Pure PS one extrusion cycle	2905	1.78	0.96	42.29	1.55 E+05
Pure PS two extrusion cycles	2751	1.78	0.96	43.19	1.53 E+05

sepiolites in the polymer matrix. However, this increase in the number of extrusion cycles could also produce a re-agglomeration of the particles deteriorating their dispersion. To determine which of the two options is dominating the behavior of these composites, formulations containing 2, 6, 8, and 10 wt% of the three different kind of sepiolites (N-SEP, O-QASEP, and O-SGSEP) were extruded one and two times and their rheological behavior was analyzed. With the aim of including figures in which data could be easily analyzed, Figure 4 only shows the data corresponding to O-QASEP. The trends for the other materials were similar and all the data for all the materials are reported in the Table 5.

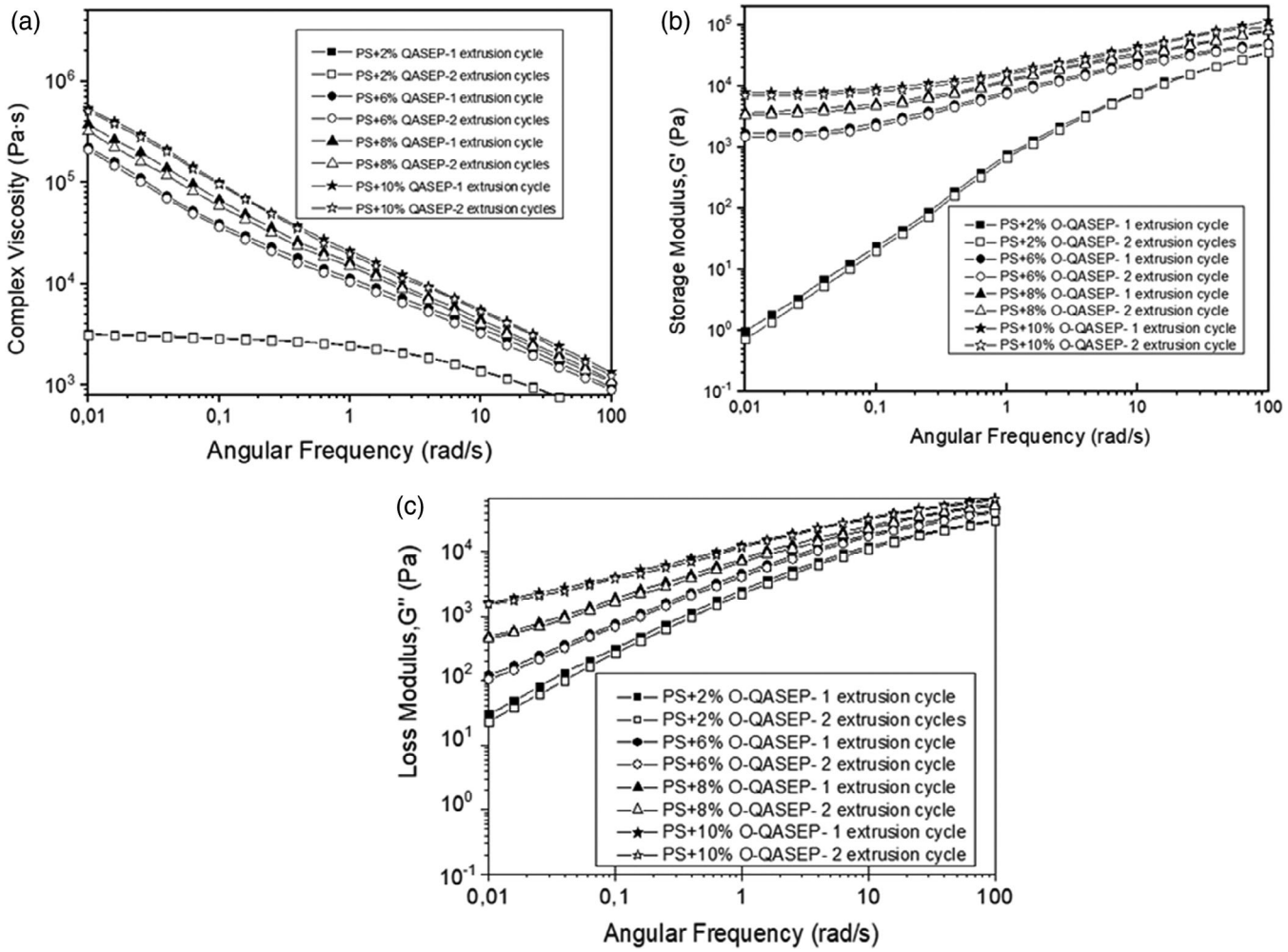

FIGURE 4 Viscoelastic properties of the formulations based on PS and O-QASEP subjected to different extrusion cycles. (a) Complex viscosity versus angular frequency. (b) Storage modulus versus angular frequency. (c) Loss modulus versus angular frequency. Common slopes values for a pure polymer are also shown in figures (b) and (c)

In both Figure 4 and Table 5, it is possible to check how the complex viscosity decreases when the number of extrusion cycles increases. For example, the reductions detected in the zero-shear viscosity due to the increment from one to two extrusion cycles for the formulations with 2 wt% of N-SEP, O-QASEP and O-SGSEP are 4% in all cases. For the formulations with 6% of N-SEP, O-SGSEP, and O-SGSEP this value is also 4%. In the previous section it was observed that for the pure PS, the reduction of the zero-shear viscosity between one and two extrusion cycles was 5%. Therefore, this reduction is very similar to the reduction detected in the polymer composites (4%). This behavior combined with the increase of the slopes of G' and G'' when changing from one to two extrusion cycles allow concluding that the main effect associated to increase the number of extrusion cycles is a deterioration of the molecular structure of the polymer matrix due to the high shear forces that are produced during the extrusion process. Another important conclusion of this analysis is that a higher number of extrusion cycles does not help to reach a better dispersion of the sepiolites in the PS matrix.

3.2 | Analysis of the dispersion degree by X-ray microtomography

In this work, another complementary technique has been employed to analyze the dispersion degree. With that purpose in mind, the formulations containing 6 wt% of the three different kinds of particles subjected to a single extrusion process, have been analyzed by X-ray microtomography. The reason for selecting these formulations is that these materials showed substantial differences in the shear dynamic rheology tests (see Figure 1 and Table 2). Figure 5 shows tomography reconstructions of the three samples. The number of particles detected is clearly lower in the composite containing 6 wt% of O-QASEP. Furthermore, the set of agglomerates detected in

TABLE 5 Linear viscoelastic properties of the formulations subjected to a different number of extrusion cycles

Sample name	Zero shear viscosity, η_0 (Pa s)	Slope of G' (Pa s)	Slope of G'' (Pa s)	Crossover frequency, ω_x (rad/s)
PS + 2% N-SEP one extrusion cycle	2916	1.48	0.97	42.26
PS + 2% N-SEP two extrusion cycle	2805	1.56	0.98	42.67
PS + 2%O-QASEP one extrusion cycle	2943	0.82	0.94	41.15
PS + 2%O-QASEP two extrusion cycle	2826	0.89	0.97	42.63
PS + 2%O-SGSEP one extrusion cycle	2912	1.52	0.98	42.89
PS + 2%O-SGSEP two extrusion cycle	2793	1.68	0.98	43.16
PS + 6% N-SEP one extrusion cycle	3839	1.27	0.95	41.18
PS + 6% N-SEP two extrusion cycle	3989	1.31	0.98	42.66
PS + 6%O-QASEP one extrusion cycle	Non-Newtonian	0.67	0.75	3.67/28.67
PS + 6%O-QASEP two extrusion cycle	Non-Newtonian	0.67	0.74	5.98//30.01
PS + 6%O-SGSEP one extrusion cycle	3498	1.32	0.92	42.16
PS + 6%O-SGSEP two extrusion cycle	3654	1.33	0.96	42.88
PS + 8% N-SEP one extrusion cycle	Non-Newtonian	0.57	0.67	2.16/25.67
PS + 8% N-SEP two extrusion cycle	Non-Newtonian	0.59	0.70	2.51/26.18
PS + 8%O-QASEP one extrusion cycle	Non-Newtonian	0.16	0.44	No crossover points
PS + 8%O-QASEP two extrusion cycle	Non-Newtonian	0.18	0.48	No crossover points
PS + 8%O-SGSEP one extrusion cycle	4726	1.15	0.89	39.24
PS + 8%O-SGSEP two extrusion cycle	4922	1.20	0.92	40.71
PS + 10% N-SEP one extrusion cycle	Non-Newtonian	0.07	0.42	No crossover points
PS + 10% N-SEP two extrusion cycle	Non-Newtonian	0.08	0.43	No crossover points
PS + 10%O-QASEP one extrusion cycle	Non-Newtonian	0.05	0.39	No crossover points
PS + 10%O-QASEP two extrusion cycle	Non-Newtonian	0.051	0.41	No crossover points
PS + 10%O-SGSEP one extrusion cycle	Non-Newtonian	0.46	0.54	2.15/23.14
PS + 10%O-SGSEP two extrusion cycle	Non-Newtonian	0.49	0.57	2.59/24.67

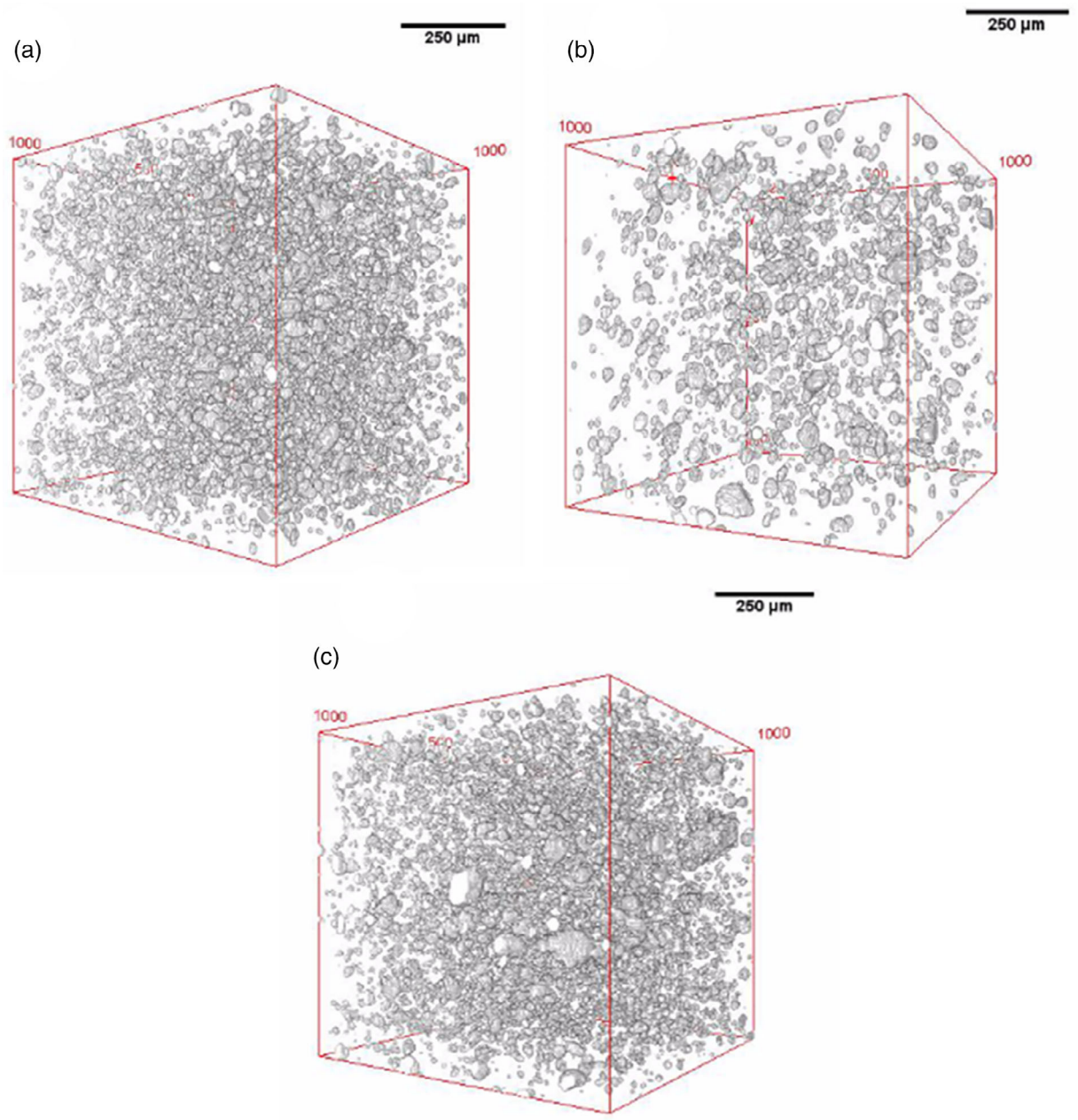

FIGURE 5 Reconstruction of the microtomography analysis for the formulations produced with 6 wt% of the different types of particles. The formulations were subjected to a single extrusion process. (a) PS + 6% N-SEP. (b) PS + 6% O-QASEP. (c) PS + 6% O-SGSEP [Color figure can be viewed at wileyonlinelibrary.com]

the materials with 6 wt% of N-SEP and 6 wt% of O-SGSEP presents a higher dimension compared to the one of the nanocomposite containing O-QASEP. As it was previously mentioned, the minimum particle size detected by the X-ray device employed is 2.5 µm and therefore, the particles detected are in fact agglomerations of individual sepiolite particles.

This behavior is a clear explanation of the different dispersion capability of the three types of particles in the polymer matrix. Figure 6 exhibits the quantitative analysis of the percentage of agglomeration of these particles, which was calculated using Equation (1).

The percentage of agglomeration, that is, the percentage of particles that are agglomerated forming agglomeration clusters bigger than 2.5 µm, is lower for the formulation containing 6 wt% of O-QASEP (41.96%) than for the materials with 6 wt% of N-SEP and 6 wt% of O-SGSEP (80.41% and 86.86%, respectively). A higher percentage of agglomeration implies a worse dispersion of the particles in the material. Therefore, the results

obtained by X-ray microtomography agree with the data obtained in the shear dynamic rheology experiments.

3.3 | Analysis of the PS based foams

This section deals with the analysis of the foaming behavior and the characteristics of the cellular structure of foams produced with the formulations containing 6 wt% of the three different types of particles. Moreover, the relationships between the dispersion degree of the particles and the cellular structure are analyzed.

3.3.1 | Gas uptake, density, and expansion ratio

The results obtained for the gas uptake, the relative density, and the expansion ratio of the cellular materials produced via gas dissolution foaming are collected in Table 6. These data indicate that the incorporation of sepiolites allows increasing the gas absorbed compared to the pure polymer. The presence of inner channels, which are able to store inside gas, together with the organo-modification that sepiolites present could make possible a higher affinity between the gas and the particles leading to a higher absorption of CO_2, compared to the formulations without nanoclays.[58] On the other hand, the relative densities and the expansion ratios are quite similar to those of the pure polymer. This fact implies that the differences in viscosity observed in the shear dynamic rheology tests do not have a significant effect in the expansion ratio of the materials. In addition, the effect of extruding the materials once or twice is not affecting the solubility and the expansion ratio.

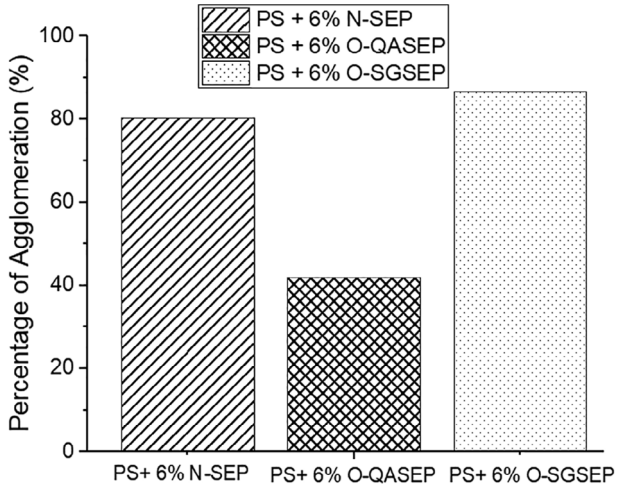

FIGURE 6 Percentage of agglomerates for the three formulations produced with the PS and 6 wt% of particles, subjected to a single extrusion cycle

3.3.2 | Cellular structure

SEM micrographs of the cellular materials produced with the pure PS and with the composites containing a fixed content (6 wt%) of the different types of sepiolites are shown in Figure 7. Several conclusions can be extracted from the qualitative and quantitative analysis of the SEM micrographs. On the one hand, when sepiolites are introduced in the PS polymer, a bi-modal behavior is detected. As it can be seen in Table 7 the volume fraction of small cells represents more than the 70% of the total volume. The large agglomerates of particles make possible the appearance of the large cells. Furthermore, as it can be seen in Table 7, the nucleation effect of sepiolites plays an essential role in the cellular structure. The cell size of the foams produced from the composites is always lower than the cell size of the foams produced from the pure PS. The lowest cell sizes are detected in the foams produced from the composites containing O-QASEP. Cell sizes as low as 13 μm have been obtained in these materials. Therefore, it seems that there is a strong connection

TABLE 6 Gas uptake, density, and expansion ratio of the cellular materials produced by the gas dissolution foaming process

Sample name	Gas uptake (wt%)	Relative density	Expansion ratio
Pure PS one extrusion cycle	7.69 ± 0.18	0.0317 ± 0.007	31.92 ± 1.06
Pure PS two extrusion cycles	7.67 ± 0.16	0.0319 ± 0.005	31.34 ± 1.04
PS + 6% N-SEP one extrusion cycle	8.19 ± 0.38	0.0303 ± 0.0063	33.00 ± 1.21
PS + 6% N-SEP two extrusion cycles	8.18 ± 0.41	0.0309 ± 0.0086	32.32 ± 1.19
PS + 6%O-QASEP one extrusion cycle	8.22 ± 0.48	0.0301 ± 0.0024	33.24 ± 0.77
PS + 6%O-QASEP two extrusion cycles	8.19 ± 0.52	0.0301 ± 0.0051	33.18 ± 0.76
PS + 6%O-SGSEP one extrusion cycle	8.15 ± 0.74	0.0311 ± 0.0040	32.08 ± 1.04
PS + 6%O-SGSEP two extrusion cycles	8.14 ± 0.66	0.0312 ± 0.0066	32.02 ± 1.16

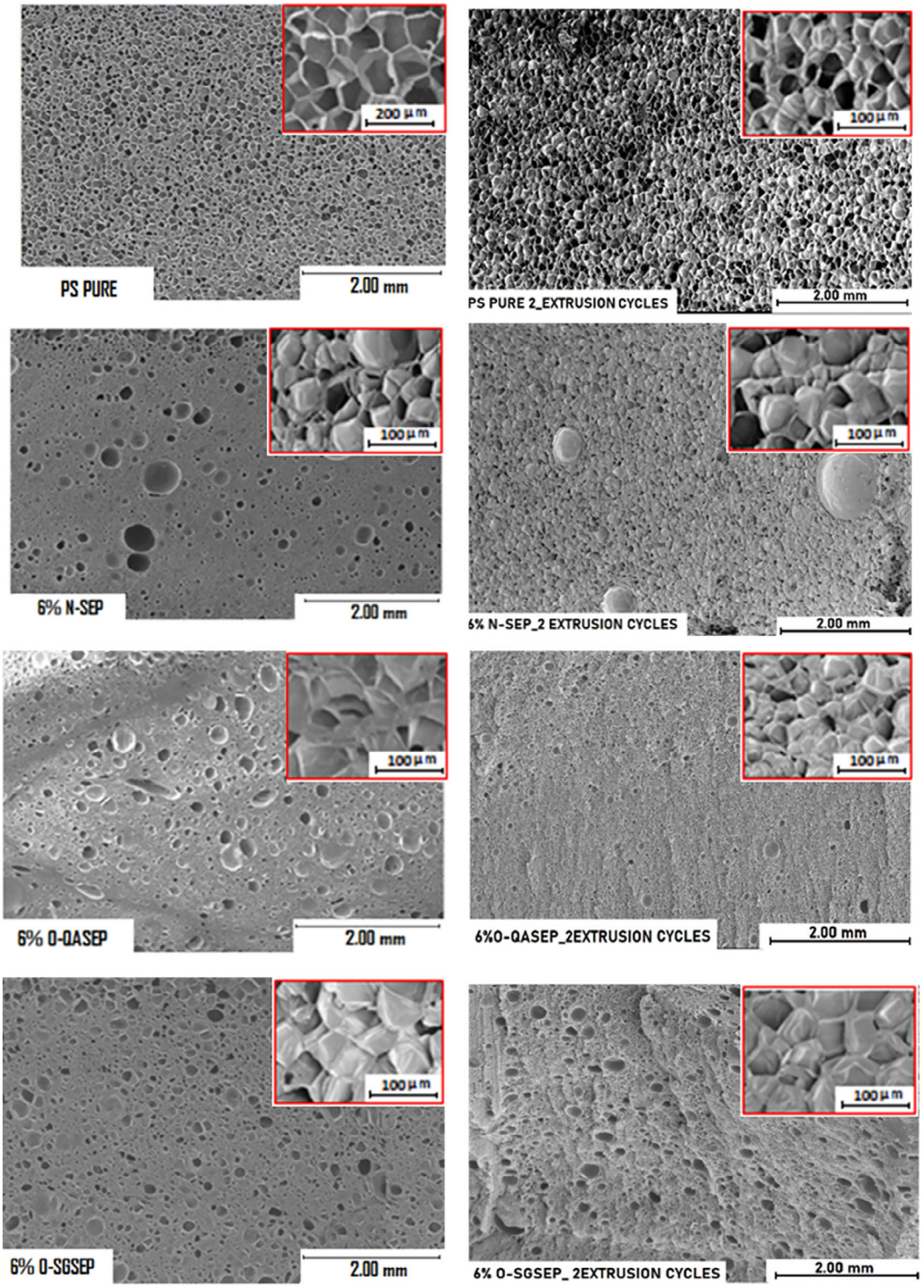

FIGURE 7 Scanning electron microscope images of the foamed samples produced with the pure PS and with the composites containing the different types of sepiolites [Color figure can be viewed at wileyonlinelibrary.com]

between the dispersion degree of the particles in the polymer matrix and their effectivity as nucleating agents. The cell size of the composites subjected to only one extrusion cycle is reduced in a 78%, 85%, and 72%, with respect to that of the polymer matrix, when using N-SEP, O-QASEP, and O-SGSEP, respectively. In the case of the composites subjected to two extrusion cycles, the cell size is reduced in a 71%, 78%, and 68%, with respect to that of the polymer matrix, when using N-SEP, O-QASEP, and O-SGSEP, respectively. In all the cases the cell size is

TABLE 7 Cell size, cell nucleation density, volume fraction of large cells, and SD/ϕ of the pure PS and the composites containing 6 wt% of the different sepiolites, subjected to one and two extrusion cycles

Sample name	Cell size (μm)	Cell nucleation density (nuclei/cm^3)	Volumetric fraction of large cells	SD/ϕ
Pure PS one extrusion cycle	88.40 ± 28.12	(4.82 ± 0.5) ·106	0.00	0.31
Pure PS two extrusion cycles	101.15 ± 34.27	(4.74 ± 0.2) ·106	0.00	0.33
PS + 6% N-SEP one extrusion cycle	19.14 ± 5.06	(3.73 ± 0.4) ·108	0.21	0.26
PS + 6% N-SEP two extrusion cycle	29.32 ± 8.09	(3.06 ± 0.4) ·108	0.18	0.30
PS + 6%O-QASEP one extrusion cycle	13.01 ± 2.69	(3.85 ± 0.1) ·108	0.18	0.20
PS + 6%O-QASEP two extrusion cycle	22.18 ± 4.79	(3.61 ± 0.2) ·108	0.15	0.21
PS + 6%O-SGSEP one extrusion cycle	24.88 ± 4.65	(3.43 ± 0.7) ·108	0.24	0.18
PS + 6%O-SGSEP two extrusion cycle	32.64 ± 7.41	(2.86 ± 0.9) ·108	0.20	0.20

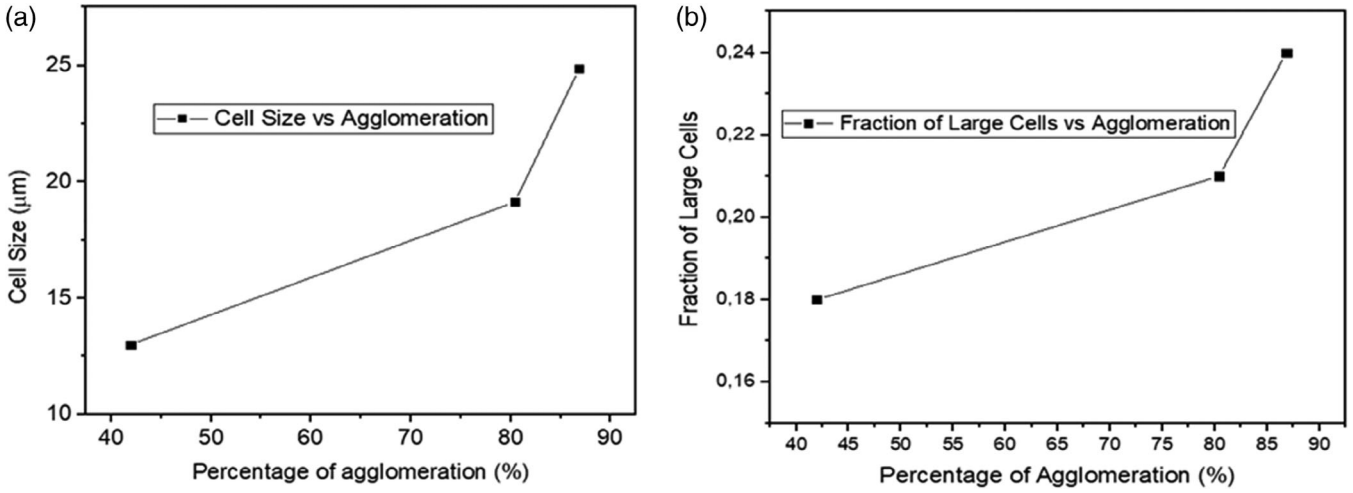

FIGURE 8 (a) Relation between the cell size and the percentage of agglomeration for formulations containing 6 wt% of sepiolites subjected to a single extrusion process. (b) Relation between the fraction of large cells and the percentage of agglomeration for materials containing 6 wt% of sepiolites subjected to a single extrusion process

higher in the samples subjected to two extrusion cycles than in the samples subjected to one extrusion cycle. This result confirms that the increment of the extrusion cycles does not improve the dispersion of the particles and therefore, the cellular structure is not improved. As the density of these materials is very similar, there is a relationship between cell size and cell nucleation density. The higher the cell size the lower the cell nucleation density. The highest value of cell nucleation density is detected in the foam containing 6 wt% of O-QASEP subjected to one extrusion cycle. The cell nucleation density of this material is 80 times higher than that of the foam produced with the pure PS.

When analyzing the relationships between the dispersion degree of the particles in the PS matrix and the characteristics of the cellular structure it is possible to conclude that the samples with the lowest percentage of aggregates, those produced with the O-QASEP, present the lowest cell sizes and the highest cell nucleation densities. This fact could indicate that the main nucleation of the small cells is related to the isolated sepiolites rather than with the agglomerations of particles. In Figure 8(a)

it is possible to see the relation between the cell size and the percentage of agglomeration for the formulations that contain 6 wt% of sepiolites subjected to a single extrusion process.

Regarding the data corresponding to the volumetric fraction of small cells depicted in Table 7, it is possible to see how samples with O-QASEP present higher percentages of small cells than the other cellular composites. This fact could be related with the better dispersibility observed of this kind of particles in the PS matrix. In other words, the bimodal behavior that appears with the sepiolites depends strongly on the agglomeration of these nanoclays. This behavior is confirmed with the Figure 8 (b), which represents the relation between the presence of large cells and the percentage of agglomeration. The higher the agglomeration ratio the higher the number of large cells that appear in the cellular structure. Finally, the ratio of the SD divided by the cell size (ϕ) gives information about the homogeneity of the cellular structure. The lower the value of SD/ϕ the more homogeneous the cellular structure. Results indicate that, when the largest cells are not considered, the structures of the foams containing sepiolites are more homogeneous than the structure of the foams produced with the pure PS. In addition, the foams produced with the formulations subjected to one extrusion cycle are also more homogeneous than the foams produced with the formulations subjected to two extrusion cycles, which agrees with the results obtained in the rheological study.

4 | CONCLUSIONS

Blends of PS with sepiolites have been prepared and characterized. The effects on the dispersion degree of the particles in the PS matrix associated to modify the type of particles (N-SEP, O-QASEP, O-SGSEP), the content of particles (2, 6, 8, and 10 wt%) and the process conditions (one and two extrusion cycles) have been analyzed in this research by using two different techniques: dynamic shear rheology and X-ray micro-computed tomography. Shear dynamic rheology results show that the O-QASEP particles are the ones with the best dispersibility. The increment detected in the complex viscosity values of the formulations containing O-QASEP and the reductions observed in the values of the slopes of G' and G'' curves are more pronounced than those observed for the other particles. Furthermore, rheological results indicate that in the formulations containing 6 wt% of O-QASEP a percolated structure has been formed; whereas it is necessary to incorporate 8 wt% of N-SEP and 10 wt% of O-SGSEP to achieve the percolation state. Moreover, the conclusions reached with the shear dynamic rheology measurements are corroborated with the X-ray micro-tomography results.

An increase of the number of extrusion cycles lead to a deterioration of the molecular structure of the PS matrix due to the high shear forces that are produced during the extrusion process. Furthermore, by increasing the number of extrusion cycles it is not possible to achieve a better dispersion of the particles in the polymer matrix.

Finally, the pure PS and the composites containing 6 wt% of sepiolites have been foamed and their cellular structure has been characterized. Results indicate that sepiolites are strong nucleating agents for PS foams Cell sizes were reduced up to 80% and cell densities were increased by 80 times. Moreover, the dispersion degree of the particles in the PS has an important effect on the cellular structure characteristics. The formulation with the best dispersion of particles (6 wt% O-QASEP) presents the lowest cell size, the highest cell density, and a very homogeneous cellular structure. In addition, the foams produced with the formulations subjected to two extrusion cycles present worse cellular structures than their counterparts subjected only to one extrusion cycle.

ACKNOWLEDGMENTS

Financial assistance from the Junta of Castile and Leon (VA202P20) and Spanish Ministry of Science, Innovation and Universities (RTI2018-098749-B-I00) and the "Ente Público Regional de la Energía de Castilla y León" (EREN) are gratefully acknowledged.

ORCID

Alberto Ballesteros https://orcid.org/0000-0003-1336-122X
Ester Laguna-Gutierrez https://orcid.org/0000-0002-3408-7816
Paula Cimavilla-Roman https://orcid.org/0000-0003-2255-973X
Maria Luisa Puertas https://orcid.org/0000-0003-3830-0263
Antonio Esteban-Cubillo https://orcid.org/0000-0003-1099-4339
Julio Santaren https://orcid.org/0000-0002-4612-2519
Miguel Angel Rodriguez-Perez https://orcid.org/0000-0002-3607-690X

REFERENCES

[1] D. L. Tomasko, A. Burley, L. Feng, S. K. Yeh, K. Miyazono, S. Nirmal-Kumar, I. Kusaka, K. Koelling, *J. Supercrit. Fluids* **2009**, *47*, 493.
[2] C. C. Ibeh, *Thermoplastic Materials: Properties, Manufacturing Methods, and Applications*, 1st ed., CRC press Taylor and Francis Group, Bocaraton **2011**.

[3] Insulation materials and their thermal properties. Greenspec, http://www.greenspec.co.uk/building-desing/insulation-materials-thermal-properties/, 2018 (accessed: March 5, 2021).
[4] A. K. Kota, B. H. Cipriano, M. K. Duesterberg, A. L. Gershon, D. Powell, S. R. Raghavan, H. A. Bruck, *Macromolecules* **2007**, *40*, 7400.
[5] V. Dolomanova, J. C. M. Rauhe, L. R. Jensen, R. Pyrz, A. B. Timmons, *J. Cell. Plast.* **2011**, *47*, 81.
[6] H. Mauroy, T. S. Plivelic, J.-P. Suuronen, F. S. Hage, J. O. Fossum, K. D. Knudsen, *Appl. Clay Sci.* **2015**, *108*, 19.
[7] L. J. Lee, C. Zeng, X. Cao, X. Han, J. Shen, G. Xu, *Compos. Sci. Technol.* **2005**, *65*, 2344.
[8] Y. Kojima, A. Usuki, M. Kawasumi, A. Okada, Y. Fukushima, T. Kurauchi, O. Kamigaito, *J. Mater. Res.* **1993**, *8*, 1185.
[9] M. Santiago-Calvo, J. Tirado-Mediavilla, J. C. Rauhe, L. R. Jensen, J. L. Ruiz-Herrero, F. Villafañe, M. A. Rodriguez-Perez, *Eur. Polym. J.* **2018**, *108*, 98.
[10] J. U. Park, J. L. Kim, D. H. Kim, K. H. Ahn, S. J. Lee, K. S. Cho, *Macromol. Res.* **2006**, *14*, 318.
[11] S. Doroudiani, M. T. Kortschot, *J. Appl. Polym. Sci.* **2003**, *90*, 1421.
[12] M. Okamoto, P. H. Nam, P. Maiti, T. Kotaka, N. Hasegawa, A. Usuki, *Nano Lett.* **2001**, *1*(6), 295.
[13] Y. Chen, R. Das, M. Battley, *Int. J. Solids Struct.* **2015**, *52*, 150.
[14] C. Zhang, B. Zhu, L. J. Lee, *Polymer (Guildf).* **2011**, *52*, 1847.
[15] X. Han, C. Zeng, L. J. Lee, K. W. Koelling, D. L. Tomasko, *Polym. Eng. Sci.* **2003**, *43*, 1261.
[16] C. Kaynak, B. M. Sipahioglu, *J. Fire Sci.* **2013**, *31*, 339.
[17] J. Shen, X. Han, L. J. Lee, *J. Cell. Plast.* **2006**, *42*, 105.
[18] Y. H. Lee, C. B. Park, K. H. Wang, M. H. Lee, *J. Cell. Plast.* **2005**, *41*, 487.
[19] G. Wang, K. L. Wang, C. J. Lu, *IOP Conf. Ser. Mater. Sci. Eng.* **2017**, *242*, 012020.
[20] W. G. Zheng, Y. H. Lee, C. B. Park, *J. Appl. Polym. Sci.* **2010**, *117*, 2972.
[21] V. Bernardo, J. Martín-de Leon, E. Laguna-Gutierrez, M. A. Rodriguez-Perez, *Eur. Polym. J.* **2017**, *96*, 10.
[22] G. Hu, F. Feng, *Polym. Technol. Mater.* **2020**, *59*, 1407.
[23] S. Bourbigot, J. W. Gilman, C. A. Wilkie, *Polym. Degrad. Stab.* **2004**, *84*, 483.
[24] E. Kontou, G. Anthoulis, *J. Appl. Polym. Sci.* **2007**, *105*, 1723.
[25] J. Yang, L. Huang, Y. Zhang, F. Chen, M. Zhong, *J. Appl. Polym. Sci.* **2013**, *130*, 4308.
[26] J. Martín-de Leon, V. Bernardo, M. A. Rodriguez-Perez, *Materials (Basel)* **2019**, *12*, 797.
[27] M. Frydrych, C. Wan, R. Stengler, K. U. O. Kelly, B. Chen, *J. Mater. Chem.* **2011**, *21*, 9103.
[28] F. Wang, J. S. Liang, Q. G. Tang, *Key Eng. Mater.* **2012**, *512-515*, 280.
[29] V. Bernardo, J. Martin-de Leon, M. A. Rodriguez-Perez, *Polym. Int.* **2019**, *68*, 1204.
[30] B. Notario, D. Velasco, M.A. Rodriguez-Perez, J. Santaren, A. Alvarez, A. Esteban-Cubillo, Int. Conf. Foam. Technol. Foam. 2012, Barcelona (Spain). **2012**, 1.
[31] F. Bergaya, B. K. Theng, G. Lagaly, *Handbook of Clay Science*, Vol. 1, Elsevier, 1st **2006**.
[32] A. Singer, E. Galán Huertos, *Developments in Palygorskite-Sepiolite Research: A New Outlook on These Nanomaterials*, 1st ed., Elsevier, Amsterdam, Netherlands **2011**.
[33] G. Tian, G. Han, F. Wang, J. Liang, *Sepiolite Nanomaterials: Structure, Properties and Functional Applications. In: Nanomaterials from Clay Minerals*, Elsevier, Amsterdam, Netherlands **2019**, p. 135.
[34] J. Zhang, S. de Juan, A. Esteban-Cubillo, J. Santarén, D.-Y. Wang, *Chinese J. Chem.* **2015**, *33*, 285.
[35] N. H. Huang, Z. J. Chen, J. Q. Wang, P. Wei, *Express Polym. Lett.* **2010**, *4*, 743.
[36] D. Killeen, M. Frydrych, B. Chen, *Mater. Sci. Eng. C.* **2012**, *32*, 749.
[37] Y. Zheng, Y. Zheng, *J. Appl. Polym. Sci.* **2006**, *99*, 2163.
[38] M. Liu, M. Pu, H. Ma, *Compos. Sci. Technol.* **2012**, *72*, 1508.
[39] S. Xie, S. Zhang, F. Wang, M. Yang, R. Séguéla, J.-M. Lefebvre, *Compos. Sci. Technol.* **2007**, *67*, 2334.
[40] D. Garcia-Lopez, J. F. Fernandez, J. C. Merino, J. Santaren, J. M. Pastor, *Compos. Sci. Technol.* **2010**, *70*, 1429.
[41] E. M. Araujo, A. M. D. Leite, R. A. da Paz, V. d. N. Medeiros, T. J. A. Melo, H. d. L. Lira, *Materials (Basel)* **2011**, *4*, 1956.
[42] Y. Yin, Z. Hong, X. Tian, Q. Zhu, H. Wang, W. Gao, *Polym. Bull.* **2018**, *75*, 2151.
[43] N. García, J. Guzmán, E. Benito, A. Esteban-Cubillo, E. Aguilar, J. Santarén, P. Tiemblo, *Langmuir* **2011**, *27*, 3952.
[44] S. K. Goel, E. J. Beckman, *Polym. Eng. Sci.* **1993**, *34*, 1137.
[45] V. Kumar, N. P. Shu, *Polym. Eng. Sci.* **1990**, *30*, 1323.
[46] K. Wang, H. Huang, J. Sheng, *J. Liq. Chromatogr. Relat. Technol.* **1998**, *21*, 1457.
[47] S. Perez-Tamarit, E. Solorzano, A. Hilger, I. Manke, M. A. Rodriguez-Perez, *Eur. Polym. J.* **2018**, *109*, 169.
[48] M. Dierick, B. Masschaele, L. Van Hoorebeke, *Meas. Sci. Technol.* **2004**, *15*, 1366.
[49] V. Bernardo, F. Loock, J. Martin-de Leon, N. A. Fleck, M. A. Rodriguez-Perez, *Macromol. Mater. Eng.* **2019**, *304*, 1900041.
[50] J. Pinto, E. Solorzano, M. A. Rodriguez-Perez, J. A. De Saja, *J. Cell. Plast.* **2013**, *49*, 555.
[51] E. Laguna-Gutierrez, R. Van Hooghten, P. Moldenaers, M. A. Rodriguez-Perez, *J. Appl. Polym. Sci.* **2015**, *132*, 1.
[52] J. Zhao, A. B. Morgan, J. D. Harris, *Polymer (Guildf)* **2005**, *46*, 8641.
[53] S. Hwan Lee, E. Cho, J. Ryoun Youn, *J. Appl. Polym. Sci.* **2007**, *103*, 3506.
[54] R. Kotsilkova, *Mech. Time-Dependent Mater.* **2002**, *6*, 283.
[55] J. Vermant, S. Ceccia, M. K. Dolgovskij, P. L. Maffettone, C. W. Macosko, *J. Rheol.* **2007**, *51*, 429.
[56] M. J. Pastoriza-Gallego, M. Pérez-Rodríguez, C. Gracia-Fernández, M. M. Piñeiro, *Soft Matter* **2013**, *9*, 11690.
[57] G. J. Nam, J. H. Yoo, J. W. Lee, *J. Appl. Polym. Sci.* **2005**, *96*, 1793.
[58] J. A. Cecilia, E. Vilarrasa-García, C. L. Cavalcante, D. C. S. Azevedo, F. Franco, E. Rodríguez-Castellón, *J. Environ. Chem. Eng.* **2018**, *6*, 4573.

How to cite this article: A. Ballesteros, E. Laguna-Gutierrez, P. Cimavilla-Roman, M. L. Puertas, A. Esteban-Cubillo, J. Santaren, M. A. Rodriguez-Perez, *J. Appl. Polym. Sci.* **2021**, e51373. https://doi.org/10.1002/app.51373